First metatarsophalangeal joint- MRI findings in asymptomatic volunteers

Dietrich, Tobias J ; da Silva, Flora L F ; de Abreu, Marcelo R ; Klammer, Georg ; Pfirrmann, Christian W A

Abstract: OBJECTIVES: To evaluate the spectrum and frequency of MR findings of the first metatarsophalangeal joint (MTPJ) in asymptomatic volunteers. METHODS: MR imaging of 30 asymptomatic forefeet was performed with a dedicated extremity 1.5-Tesla system. Participants were between 20 and 49 years of age (mean ± SD: 35.5 ± 8.4 years). Two radiologists assessed cartilage, bone, capsuloligamentous structures, and tendons of first MTPJs on MR images. RESULTS: Cartilage defects were observed in 27 % (n = 8) of first MTPJs, most frequently located at the base of the proximal phalanx (23 %, n = 7), whereas cartilage defects of the metatarsal head (13 %, n = 4) and the metatarsosesamoid compartment were rare (0 %-3 %, n = 0-1). Bone marrow oedema-like signal changes were present in 37 % (n = 11) and subchondral cysts in 20 % (n = 6) of first MTPJs. Hyperintense areas on intermediate-weighted sequences (range: 30-43 %, n = 9-13) and on fluid-sensitive sequences with fat suppression (range: 33-60 %, n = 10-18) within the medial and lateral collateral ligament complex were common. Plantar recesses (77 %, n = 23) and distal dorsal recesses (87 %, n = 26) were frequently observed. CONCLUSIONS: Cartilage defects, bone marrow oedema-like signal changes, subchondral cysts, plantar recesses, and distal dorsal recesses were common findings on MRI of first MTPJs in asymptomatic volunteers. The collateral ligaments were often heterogeneous in structure and showed increased signal intensity. KEY POINTS: • Cartilage defects of asymptomatic first metatarsophalangeal joints were common on MRI. • The collateral ligaments were often heterogeneous in structure and showed increased signal intensity. • Areas of increased signal intensity within the flexor and extensor tendons were rare. • These observations need to be considered in MR examinations of symptomatic cases.

DOI: https://doi.org/10.1007/s00330-014-3489-y

Eur Radiol (2015) 25:970–979
DOI 10.1007/s00330-014-3489-y

MUSCULOSKELETAL

First metatarsophalangeal joint- MRI findings in asymptomatic volunteers

Tobias Johannes Dietrich · Flora Luciana Figueira da Silva · Marcelo Rodrigues de Abreu · Georg Klammer · Christian W. A. Pfirrmann

Received: 27 May 2014 / Revised: 20 August 2014 / Accepted: 4 November 2014 / Published online: 21 November 2014

Abstract
Objectives To evaluate the spectrum and frequency of MR findings of the first metatarsophalangeal joint (MTPJ) in asymptomatic volunteers.
Methods MR imaging of 30 asymptomatic forefeet was performed with a dedicated extremity 1.5-Tesla system. Participants were between 20 and 49 years of age (mean±SD: 35.5± 8.4 years). Two radiologists assessed cartilage, bone, capsuloligamentous structures, and tendons of first MTPJs on MR images.
Results Cartilage defects were observed in 27 % (n=8) of first MTPJs, most frequently located at the base of the proximal phalanx (23 %, n=7), whereas cartilage defects of the metatarsal head (13 %, n=4) and the metatarsosesamoid compartment were rare (0 %–3 %, n=0-1). Bone marrow oedema-like signal changes were present in 37 % (n=11) and subchondral cysts in 20 % (n=6) of first MTPJs. Hyperintense areas on intermediate-weighted sequences (range: 30–43 %, n=9–13) and on fluid-sensitive sequences with fat suppression (range: 33–60 %, n=10–18) within the medial and lateral collateral ligament complex were common. Plantar recesses (77 %, n=23) and distal dorsal recesses (87 %, n=26) were frequently observed.
Conclusions Cartilage defects, bone marrow oedema-like signal changes, subchondral cysts, plantar recesses, and distal dorsal recesses were common findings on MRI of first MTPJs in asymptomatic volunteers. The collateral ligaments were often heterogeneous in structure and showed increased signal intensity.

Key Points
- *Cartilage defects of asymptomatic first metatarsophalangeal joints were common on MRI.*
- *The collateral ligaments were often heterogeneous in structure and showed increased signal intensity.*
- *Areas of increased signal intensity within the flexor and extensor tendons were rare.*
- *These observations need to be considered in MR examinations of symptomatic cases.*

Keywords Magnetic resonance imaging · Forefoot. Metatarsophalangeal joint · Asymptomatic · Volunteers

Abbreviations

EHL	Extensor hallucis longus tendon
ETL	Echo train length
Fat-sup	Fat suppression
FOV	Field of view
FSE	Fast spin-echo
ICC	Intraclass correlation coefficient
IW	Intermediate-weighted
MTPJ	Metatarsophalangeal jointl
NSA	Number of signals acquired

T. J. Dietrich (✉) · F. L. F. da Silva · C. W. A. Pfirrmann
Radiology, Orthopedic University Hospital Balgrist, University of Zurich, Forchstrasse 340, 8008 Zurich, Switzerland
e-mail: tobiasjdietrich@gmail.com

F. L. F. da Silva
e-mail: florafs@terra.com.br

C. W. A. Pfirrmann
e-mail: Christian.Pfirrmann@balgrist.ch

F. L. F. da Silva · M. R. de Abreu
Radiology, Hospital Mãe de Deus and Mãe de Deus Center, Rua José de Alencar 286, Porto Alegre, RS, Brazil

M. R. de Abreu
e-mail: marcelorad@gmail.com

G. Klammer
Orthopedic Surgery, Orthopedic University Hospital Balgrist, University of Zurich, Forchstrasse 340, 8008 Zurich, Switzerland
e-mail: georg@klammer.ch

SD	Standard deviation
STIR	Short-Tau inversion recovery
T1-w	T1-weighted
TE	Echo time
TI	Inversion time
TR	Repetition time

Introduction

Forefoot pain related to disorders of the first metatarsophalangeal joint is a true diagnostic challenge in view of the numerous painful conditions that cause symptoms [1–7]. While MRI of the forefoot plays an important role in the diagnostic workup, a broad spectrum of findings might be observed between normal [8–11] and abnormal MRI morphology of the first metatarsophalangeal joint (MTPJ), including cartilage defects, bone marrow oedema-like signal changes, subchondral cysts, recesses of the plantar plate, and heterogeneous structures and hyperintense areas of the capsuloligamentous structures. These incidental MRI findings in the absence of corresponding clinical symptoms may be diagnostically misleading. Investigators have hypothesized that several incidental and potential misleading MRI findings of the first metatarsophalangeal joint without clinical relevance may be frequently observed on images of a clinical standard MR protocol of the forefoot.

Theumann et al. [8] presented the anatomy of 12 first MTP joints of cadavers on MR images. There is no data in the literature that addresses the typical morphology of the first MTP joint on MR images in a larger cohort of asymptomatic individuals. Thus the purpose of the present study was to evaluate the spectrum and frequency of MR findings of the first metatarsophalangeal joint in asymptomatic volunteers.

Materials and methods

Study population

Approval of the present prospective study by the responsible institutional review board and signed informed consent of all volunteers was obtained prior to the MR imaging examinations. Subjects meeting the inclusion criteria were between 20 and 49 years of age, with no symptoms or medical history of pain in the examined foot. Exclusion criteria included symptoms in the evaluated side of the foot, previous fracture, previous joint dislocation, previous tear in muscles or ligaments, previous surgery of the forefoot, diabetes mellitus, rheumatic disorders, history of neoplasm, pregnancy, and contraindications for MRI, which were assessed based on patient questionnaire responses. Thirty asymptomatic volunteers were included in the present investigation. The parameters of the study population are summarized in Table 1.

Imaging protocol

All MR images were acquired with a dedicated extremity 1.5-Tesla MRI (Optima MR430s, GE Healthcare, Waukesha, WI, USA). Volunteers were examined in a prone position. An MRI forefoot protocol consisting of seven sequences was employed, as shown in Table 2. Three of the seven sequences were centred on the first MTPJ. Four sequences covered the whole forefoot and included all five MTP joints.

MR image analysis

Two musculoskeletal radiologists, both with three years of musculoskeletal radiology experience, evaluated the MR images. Quantitative analysis was performed using electronic calipers on a picture archiving and communication system workstation (Impax 6, Agfa HealthCare, Mortsel, Belgium).

The following morphologic parameters of the first MTPJ were analyzed:

Cartilage, Bone Marrow Oedema-Like Signal Changes, and Subchondral Cysts

The frequency and size of areas with cartilage defects were assessed for the head of the first metatarsal bone, base of the first proximal phalanx, medial and lateral sesamoid bone, as well as medial and lateral sesamoid facet of the first metatarsal bone. The frequency and size in two dimensions of bone marrow oedema-like signal changes and subchondral cysts were analyzed for the head of the first metatarsal bone, base of the first proximal phalanx, medial and lateral sesamoid bone, medial and lateral sesamoid facet of the first metatarsal bone, and the origin of medial and lateral collateral ligaments.

Collateral Ligament Complex and Intersesamoid Ligament

The medial, accessory medial, lateral, accessory lateral collateral ligament, and intersesamoid ligament were investigated for the following parameters: thickness of the collateral and

Table 1 Study population: 30 asymptomatic volunteers were included; 10 volunteers of each gender were 20–29, 30–39, and 40–49 years of age

Number of volunteers (*n*)	Total 30	Male 14	Female 16
Right (*n*)	18	8	10
Left (*n*)	12	6	6
Mean age±SD (years)	35.5±8.4	35.6±8.1	35.5±8.9

Table 2 MRI sequence parameters

	Sequences centred to the first MTPJ			Sequences covering all five MTP joints			
	Transverse IW FSE	Sagittal IW FSE fat-sup	Coronal IW FSE	Transverse IW FSE fat-sup	Transverse T1-w FSE	Sagittal T1-w FSE	Coronal STIR FSE sequence
TR/TE/TI (msec)	2000/8.3	2000/21	2000/25.8	2223/26.6	648/9.9	578/11.3	3500/32.4/110
NSA	4	4	4	4	4	3	2
FOV (mm)	60	80	80	100	100	100	120
Matrix	320×224	420×288	320×224	320×224	420×320	384×320	320×224
Section thickness (mm)	3	2.5	2.5	3	3	3	2
Sections per slab	14	12	12	14	14	22	16
Acquisition time (min)	5:38	6:01	5:49	5:08	5:00	5:08	5:25
ETL	9	9	9	9	4	4	9

IW intermediate-weighted, *FSE* fast spin-echo, *fat-sup* fat-suppression, *T1-w* T1-weighted, *STIR* short-Tau inversion recovery, *TR* repetition time, *TE* echo time, *TI* inversion time, *NSA* number of signals acquired, *FOV* field of view, *ETL* echo train length

intersesamoid ligaments, definition of the inner and outer contour, the signal compared to muscle signal on all sequences, the presence of hyperintense areas on fluid-sensitive sequences with fat suppression as STIR and intermediate-weighted MR images with fat suppression, and the structure of the ligament as either homogeneous or heterogeneous.

Tendons

The transverse dimensions and signal of the extensor hallucis longus tendon, extensor hallucis brevis tendon, flexor hallucis longus tendon, and abductor hallucis tendon were analyzed. Lateralization of the extensor hallucis longus tendon (EHL) was quantified as the distance between the dorsoplantar midline of the first metatarsal head and the centre of the EHL tendon on transverse T1-weighted MR images, as shown in Fig. 1.

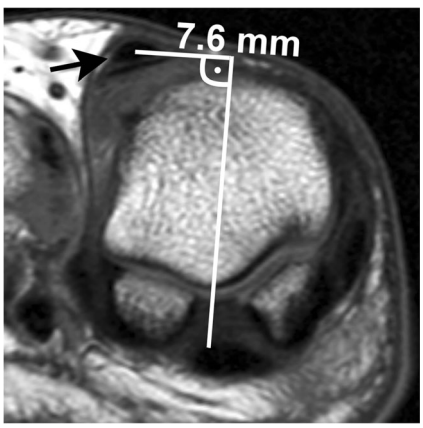

Fig. 1 28-year-old woman. Lateralization of the extensor hallucis longus tendon (*arrow*) (EHL) was quantified as the distance (7.6 mm) between the dorsoplantar midline of the first metatarsal head and the centre of the EHL tendon on transverse T1-weighted MR images

Sesamoid Bones

The position of the medial and lateral sesamoid bones on transverse IW MR images was assessed using a classification previously described [4, 12]. Medial sesamoids entirely medial to the intersesamoid ridge were considered as no subluxation. Less than 50 % overlap of the medial sesamoid relative to the intersesamoid ridge and less than 50 % overlap of the lateral sesamoid relative to the lateral facet of the first metatarsal head was considered as subluxation. In addition, the following parameters of the medial and lateral sesamoid bones were obtained: presence of bipartite or multipartite sesamoid bones, presence of sclerosis as low signal intensity on all MR image sequences, and the size of the sclerosis in two dimensions.

Miscellaneous Parameters

The presence and depth of a distal central recess of the plantar plate and a distal dorsal recess, both located at the insertion of the capsuloligamentous structures at the base of the first proximal phalanx, were evaluated. The presence and dimension of a dorsal plica at the insertion of the joint capsule at the base of the first proximal phalanx and bursa of the first intermetatarsal space were determined. In addition, flattening of the first metatarsal head and the presence of joint effusion and osteophytes, including their location, were analyzed. The diagnostic criterion for joint effusion of the first metatarsophalangeal joint on MRI was defined as fluid-equivalent signal intensity within the joint, with apparent distension of the joint capsule.

Statistical analysis

Mean and standard deviation values were calculated for quantitative parameters, and the frequency of qualitative

Table 3 MRI findings of cartilage, bone marrow oedema-like signal changes (used simplification: bone marrow oedema) and subchondral cysts

	Cartilage defects	Bone marrow oedema	Subchondral cysts
	Mean±SD	Mean±SD	Mean±SD
1st MTP - Lesion size (mm)	2.5±1.2×2.0±1.3	5.8±2.5×4.1±1.8	3.1±1.7×2.6±1.4
	Percentage	Percentage	Percentage
1st MTP Overall lesion frequency	27 % (*n*=8)	37 % (*n*=11)	20 % (*n*=6)
Lesion frequency of each compartment			
1st Metatarsal head	13 % (*n*=4)	7 % (*n*=2)	0 % (*n*=0)
1st Phalanx	23 % (*n*=7)	17 % (*n*=5)	7 % (*n*=2)
Medial sesamoid bone	0 % (*n*=0)	10 % (*n*=3)	0 % (*n*=0)
Lateral sesamoid bone	3 % (*n*=1)	10 % (*n*=3)	0 % (*n*=0)
Medial facet	0 % (*n*=0)	3 % (*n*=1)	0 % (*n*=0)
Lateral facet	0 % (*n*=0)	0 % (*n*=0)	3 % (*n*=1)
Origin medial collateral ligament	not applicable	10 % (*n*=3)	10 % (*n*=3)
Origin lateral collateral ligament	not applicable	0 % (*n*=0)	0 % (*n*=0)

Values are presented as mean±SD and percentages. Absolute numbers of each positive MRI finding of 30 volunteers are given in parentheses

parameters was calculated as its percentage and absolute values. The values of one assessment are given throughout the manuscript, including tables. Interobserver agreement regarding quantitative measurements was assessed using the intraclass correlation coefficient (ICC), and qualitative (categorical) parameters were assessed using Cohen's kappa coefficient [13, 14].

ICC and kappa values less than 0.20 were rated as slight agreement, between 0.21 and 0.40 as fair agreement, between 0.41 and 0.60 as moderate agreement, between 0.61 and 0.80 as good agreement, and between 0.81 and 1.00 as very good interobserver agreement [13, 15]. The Student's t test served for comparison of the thickness of the medial and lateral collateral ligament complex. A software package was used for statistical analysis (SPSS Statistics for Windows Version 21.0, IBM Corp, Armonk, NY, USA).

Fig. 2 25-year-old male volunteer. A small cartilage defect (*open arrow*) with an associated small area of bone marrow oedema-like signal changes (*arrow*) of the base of the left first proximal phalanx on a coronal STIR image

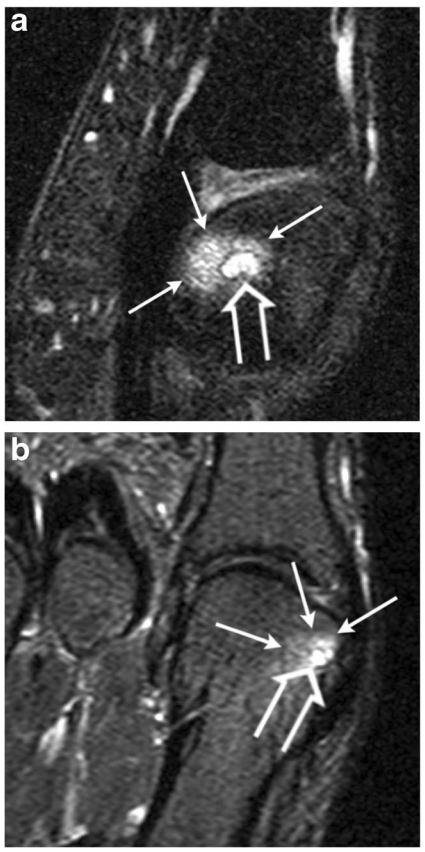

Fig. 3 27-year-old male volunteer with bone marrow oedema-like signal changes (*arrows*) and subchondral cysts (*open arrows*) at the origin of the medial collateral ligament complex on fat-suppressed sagittal intermediate-weighted (*A*) and coronal STIR MR images (*B*)

Results

Cartilage, bone marrow oedema-like signal changes and subchondral cysts

Cartilage defects were observed in 27 % of the first MTP joints (Table 3). The most frequent location for cartilage defects was the base of the proximal phalanx (Fig. 2). Cartilage defects of the first metatarsal head (13 %) and in the metatarsosesamoid compartment were rare (0 %–3 %). Small areas of bone marrow oedema-like signal changes were present in 37 % (Figs. 2 and 3). The most frequent location was the base of the proximal phalanx. Subchondral cysts were detectable in 20 % of the first MTP joints, most frequently at the origin of the medial collateral ligament (Fig. 3).

Collateral ligament complex and intersesamoid ligament

The ligament thickness was 2.3±0.7 mm for the accessory lateral collateral ligament and 2.9±0.8 mm for the accessory medial collateral ligament (Table 4). The medial collateral ligament complex was thicker than the lateral collateral ligament complex, with a statistically significant difference for the accessory collateral ligaments (2.9±0.8 mm versus 2.3±0.7 mm, $p<0.002$), whereas no significant difference was noted between the thickness of the medial and lateral collateral ligaments (2.6±0.6 mm versus 2.4±0.8 mm, $p=0.48$).

Most of the ligaments of the medial and lateral collateral ligament complex were hypointense on intermediate-weighted and T1-weighted sequences compared to the signal of the muscle (range: 57–100 %). However, hyperintense areas on intermediate-weighted sequences (range: 30–43 %) and on fluid-sensitive sequences with fat suppression (range: 33–60 %) within the collateral ligament complex were common (Figs. 4 and 5). The collateral ligaments were often heterogeneous in structure and showed increased signal intensity. A heterogeneous structure of the collateral ligament complex was observed in a range between 63 % for the accessory medial collateral ligament and 73 % for both ligaments of the lateral collateral ligament complex.

The intersesamoid ligament demonstrated a thickness of 3.1±0.5 mm and was predominantly hypointense on intermediate-weighted and T1-weighted MR images (Fig. 6). Hyperintense areas on fluid-sensitive sequences with fat suppression were detected infrequently, in 10 % of the analyzed intersesamoid ligaments.

Tendons

The extensor hallucis longus tendon, extensor hallucis brevis tendon, flexor hallucis longus tendon, and abductor hallucis tendon were almost always hypointense (range: 93–100 %). A homogeneous tendon structure was almost always noted on the evaluated MR images (Table 5). The lateralization of the extensor hallucis longus tendon as the distance between the midline of the first metatarsal head and the centre of the EHL tendon was 7.1±1.9 mm.

Table 4 MRI findings of the collateral ligament complex and intersesamoid ligament

	Medial collateral ligament	Accessory medial collateral ligament	Lateral collateral ligament	Accessory lateral collateral ligament	Intersesamoid ligament
	Mean±SD	Mean±SD	Mean±SD	Mean±SD	Mean±SD
Thickness (mm)	2.6±0.6	2.9±0.8	2.4±0.8	2.3±0.7	3.1±0.5
	Percentage	Percentage	Percentage	Percentage	Percentage
Good definition of the ligament					
Inner contour	77 % (*n*=23)	77 % (*n*=23)	87 % (*n*=26)	63 % (*n*=19)	80 % (*n*=24)
Outer contour	83 % (n=25)	97 % (*n*=29)	77 % (*n*=23)	60 % (*n*=18)	87 % (*n*=26)
Intermediate-weighted sequence					
Hyperintense areas within ligament	40 % (*n*=12)	40 % (*n*=12)	43 % (*n*=13)	30 % (*n*=9)	0 % (*n*=0)
Isointense areas within ligament	87 % (*n*=26)	80 % (*n*=24)	87 % (*n*=26)	93 % (*n*=28)	40 % (*n*=12)
Hypointense areas within Ligament	97 % (n=29)	100 % (*n*=30)	70 % (*n*=21)	90 % (*n*=27)	90 % (*n*=27)
T1-weighted Sequence					
Isointense areas within ligament	90 % (*n*=27)	80 % (*n*=24)	87 % (*n*=26)	93 % (*n*=28)	53 % (*n*=16)
Hypointense areas within ligament	97 % (*n*=29)	93 % (*n*=28)	57 % (*n*=17)	87 % (*n*=26)	90 % (*n*=27)
Hyperintense areas on fluid-sensitive fat suppressed Sequences	40 % (*n*=12)	33 % (*n*=10)	57 % (*n*=17)	60 % (*n*=18)	10 % (*n*=3)
Heterogeneous structure of ligament	70 % (*n*=21)	63 % (*n*=19)	73 % (*n*=22)	73 % (*n*=22)	57 % (*n*=17)

Values are presented as mean±SD and percentages. Absolute numbers of each positive MRI finding of 30 volunteers are given in parentheses

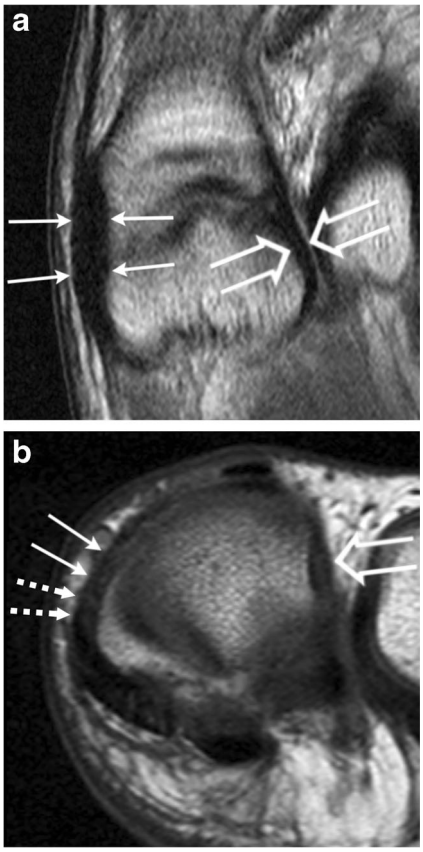

Fig. 4 37-year-old male volunteer with hypointense medial and lateral collateral ligament complex. The medial accessory medial collateral ligament (*arrows*) and accessory lateral collateral ligament (*open arrows*) demonstrate purely hypointense signal characteristics on a coronal intermediate-weighted MR image (*A*). The medial collateral ligament (*arrows*), accessory medial collateral ligament (*dotted arrows*) and lateral collateral ligament (*open arrow*) is hypointense on a transverse T1-weighted MR image (*B*)

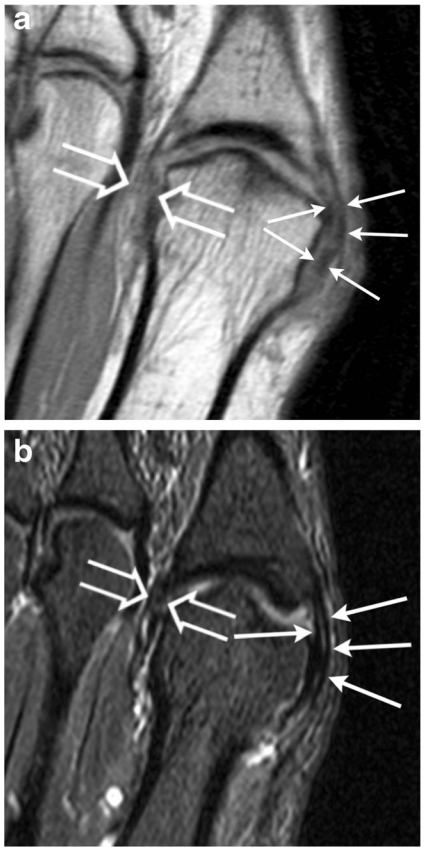

Fig. 5 47-year-old female volunteer with heterogeneous signal of the collateral ligament complex. The medial collateral ligament (*arrows*) and lateral collateral ligament (*open arrows*) demonstrate hypointense, isointense, and hyperintense areas on a coronal intermediate-weighted MR image (*A*). The accessory medial collateral ligament (*arrows*) and accessory lateral collateral ligament (*open arrows*) show hyperintense areas on the coronal STIR MR image (*B*)

Sesamoid bones

Lateral subluxation of the medial and lateral sesamoid bones was not observed in any volunteer. A bipartite medial sesamoid was noted in four of the 30 (13 %) volunteers, and bone marrow oedema-like signal changes were detected in three of four bipartite medial sesamoid bones (Table 6). No bipartite lateral sesamoid was identified. Sclerosis of the medial sesamoid was observed in 20 %, with a mean size of 6.1±2.1×3.7 ±1.3 mm. The frequency of sclerosis of the lateral sesamoid was 7 %, with a mean size of 4.8±1.5×4.2±2.0 mm.

Miscellaneous parameters

A distal central recess of the plantar plate at the insertion of the capsuloligamentous structures at the base of the first proximal phalanx, with a mean depth of 2.2±0.6 mm (Table 7), was seen in 77 % of the volunteers. A distal dorsal recess at the insertion of the joint capsule at the base of the first proximal phalanx, with a mean depth of 3.9±0.9 mm (Fig. 7), was observed in 87 % of the volunteers. A dorsal plica at the insertion of the joint capsule at the base of the first proximal phalanx, with a mean size of 1.1±0.3 mm, was visible in 43 % of the volunteers. A bursa within the first intermetatarsal space, with a mean size of 1.4±0.4 mm, was determined in 47 % of subjects.

Flattening of the first metatarsal head was not observed in any of the 30 volunteers. A joint effusion was noted in three volunteers. No osteophytes were detected in any of the 30 MTP joints.

Interobserver agreement

ICC values were used to assess interobserver agreement between reader 1 and reader 2 with regard to quantitative measurements. ICC values ranged from 0.43 for the size of the bursa within the first intermetatarsal space to 0.99 for the dimensions of sclerosis of the lateral sesamoid, rated as interobserver agreement from moderate to very good. Most ICC values were rated as good (n=12) or very good (n=12)

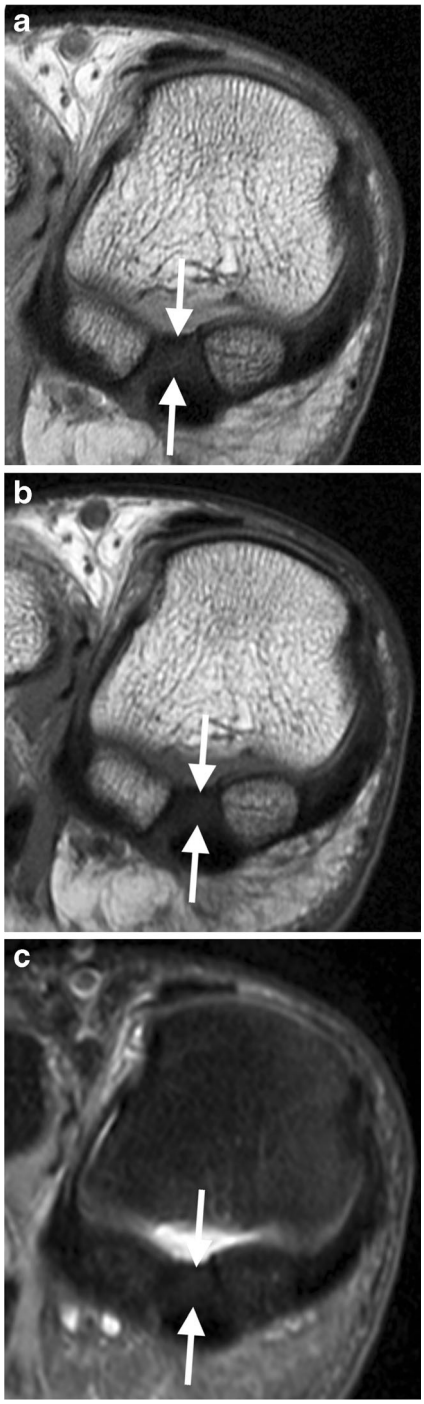

Fig. 6 27-year-old male volunteer. *Arrows* indicate the visible inner and outer contour of the intersesamoid ligament. The demonstrated intersesamoid ligament is hypointense on intermediate-weighted (*A*) and T1-weighted (*B*) MR images. No hyperintense areas are visible on the transverse intermediate-weighted MR image with fat suppression (*C*)

interobserver agreement for quantitative measurement. Cohen's kappa coefficient values served for the assessment of interobserver agreement between reader 1 and reader 2 with regard to qualitative measurements. Kappa values ranged from 0.36 for the presence of isointense areas on T1-weighted MR images within the intersesamoid ligament to 1.0 for the presence of hypointense areas on T1-weighted MR images within the medial collateral ligament, rated as interobserver agreement from fair to very good. Most Kappa values were rated as good (n=24) interobserver agreement.

Discussion

The present investigation confirmed the hypothesis that many aberrant MRI findings are present in asymptomatic first MTPJs. The most interesting findings were that cartilage defects and subchondral cysts occurred in approximately one-fifth of the first MTPJs on MR images in asymptomatic participants. Bone marrow oedema-like signal changes and signal alterations of the collateral ligament complex were found with an intermediate frequency. A heterogeneous structure of the collateral ligament complex was common. Such findings could have a higher prevalence in an older study population with a higher frequency of osteoarthritis. However, an age range of between 20 and 49 years was chosen for the study population in order to avoid selection bias due to a potential high frequency of degenerative findings on MR images.

Normal findings on clinical examination and medical imaging of the plantar plate and periarticular structures of the first metatarsophalangeal joint have recently attracted increased interest among orthopaedic foot surgeons [16–19]. Approximately 50 % of the body weight transmits through the first MTP joint during gait, and may reach eight times the body weight during running and jumping. The plantar plate of the first MTPJ has been identified as an integral component of the capsuloligamentous complex. Thus the plantar plate provides stability to the first MTPJ, and consequently, injuries to the plantar plate and capsuloligamentous complex may result in functional disability [16–19].

First MTP joint pain has a broad differential diagnosis as capsuloligamentous injuries, including turf toe, radiographically occult fractures, sesamoiditis, osteochondral lesions, bursitis, plantar fibromatosis, osteomyelitis, neuropathic osteoarthropathy, osteoarthritis, tendinosis, tendon tears, tenosynovitis, gout, and rheumatoid arthritis [1–7, 16]. MRI is a powerful imaging technique that may be used for confirmation of clinical and radiographic diagnosis [1, 20]. The broad differential diagnosis of first MTP joint pain and the high prevalence of incidental findings of the first metatarsophalangeal joint in asymptomatic participants on MR images could result in false-positive conclusions in symptomatic cases, with potentially inefficient treatment.

In the present investigation, the base of the first proximal phalanx revealed more cartilage defects than the head of the first metatarsal bone, while cartilage defects in the

Table 5 MRI findings of the extensor hallucis longus tendon, extensor hallucis brevis tendon, hallucis longus tendon, and abductor hallucis tendon

		Extensor hallucis longus tendon	Extensor hallucis brevis tendon	Flexor hallucis longus tendon	Abductor hallucis tendon
		Mean±SD	Mean±SD	Mean±SD	Mean±SD
Thickness (mm)		5.0±1.2×1.8±0.4	4.0±1.1×0.9±0.3	6.8±1.0×3.0±0.6	7.7±1.1×2.5±0.5
		Percentage	Percentage	Percentage	Percentage
Intermediate-weighted sequence					
Hyperintense areas within tendon	0 % (*n*=0)	0 % (*n*=0)	0 % (*n*=0)	0 % (*n*=0)	
Isointense areas within tendon	0 % (*n*=0)	0 % (*n*=0)	0 % (*n*=0)	0 % (*n*=0)	
Hypointense areas within tendon	100 % (*n*=30)	100 % (*n*=30)	100 % (*n*=30)	100 % (*n*=30)	
T1-weighted sequence					
Isointense areas within tendon	0 % (*n*=0)	0 % (*n*=0)	3 % (*n*=1)	3 % (*n*=1)	
Hypointense areas within tendon	100 % (*n*=30)	100 % (*n*=30)	100 % (*n*=30)	97 % (*n*=29)	
Hyperintense areas on fluid-sensitive fat-suppressed sequences	0 % (*n*=0)	7 % (*n*=2)	0 % (*n*=0)	0 % (*n*=0)	
Heterogeneous structure	0 % (*n*=0)	0 % (*n*=0)	3 % (*n*=1)	7 % (*n*=2)	

Values are presented as mean±SD and percentages. Absolute numbers of each positive MRI finding of 30 volunteers are given in parentheses

metatarsosesamoid compartment were rarely observed. This is in contrast to previously published data [21–23] on cadavers and intraoperative findings in patients. The most frequent location of cartilage defects of the first MTPJ in the literature were described at the head of the first metatarsal bone and the sesamoid bones [21–23]. However, the surgical data may be biased by differences in accessibility of various joint compartments during hallux valgus reconstruction.

In a study yielding results similar to those of the present study, Theumann et al. [8] noted a thicker medial collateral ligament in comparison to the lateral collateral ligament of MTPJs of the great toe in 12 cadavers. The authors reported thickness of the collateral ligament complex from 2.1 mm for the lateral collateral ligament and 3.1 mm for the medial lateral ligament in cadavers [8]; these data are similar to those of asymptomatic volunteers in the present study.

Tendons demonstrate low-signal-intensity characteristics on IW and T1-weighted images in the majority of cases. Signals of the tendons included in the study were primarily homogeneous hypointense. As such, tendinosis and partial tears might be diagnosed in tendons of the first MTPJ with hyperintense areas on MR images insofar as they are not related to a magic-angle artefact. Diameter changes in tendons might be additional diagnostic criteria for tendinopathy [1, 24, 25].

Table 6 MRI findings of the medial and lateral sesamoid bones

	Medial sesamoid	Lateral sesamoid
	Percentage	Percentage
Lateral subluxation	0 % (*n*=0)	0 % (*n*=0)
Bipartite	13 % (*n*=4)	0 % (*n*=0)
Sclerosis	20 % (*n*=6)	7 % (*n*=2)
	Mean±SD	Mean±SD
Sclerosis size (mm)	6.1±2.1×3.7±1.3	4.8±1.5×4.2±2.0

Values are presented as percentages and mean±SD

Absolute numbers of each positive MRI finding of 30 volunteers are given in parentheses

Frankel and Harrington [26] postulated a high prevalence of symptomatic partite sesamoids. Thus, a diagnostic challenge might be to differentiate between a bipartite sesamoid with stress response and a unipartite sesamoid with a suspected fracture and/or pseudarthrosis [5, 11]. Fluid signals between the two bone fragments may be seen in the case of both pseudarthrosis and fracture [11]. Nwawka et al. [5] suggested that MRI could show bone marrow oedema-like signal changes in a recently fractured sesamoid, whereas bipartite medial sesamoids present without MRI signal abnormality. These signal changes may not be effective as specific markers with which to differentiate fractured unipartite hallucal sesamoids and asymptomatic and symptomatic bipartite hallucal sesamoids, however, as we found bone marrow oedema-like signal changes in 75 % (3/4) of the bipartite medial sesamoids in asymptomatic participants. A comparison between MR imaging and histologic findings in osteoarthritic knees revealed that a bone marrow oedema pattern on MRI represented various non-characteristic histological abnormalities, including bone marrow necrosis, bone marrow fibrosis, and trabecular abnormalities, but represented only a small volume of bone marrow oedema [27]. Thus, throughout the present manuscript, hyperintense areas on fluid-sensitive sequences with fat suppression and corresponding areas with low signal intensity on T1-weighted images are described as bone marrow oedema-like signal changes.

Table 7 MRI findings of the plantar recess, distal dorsal recess, dorsal plica and bursa within the first intermetatarsal space

	Plantar recess	Distal dorsal recess	Dorsal plica	Bursa
	Percentage	Percentage	Percentage	Percentage
Good definition	77 % (*n*=23)	87 % (*n*=26)	43 % (*n*=13)	47 % (*n*=14)
	Mean±SD	Mean±SD	Mean±SD	Mean±SD
Depth	2.2±0.6	3.9±0.9	1.1±0.3	1.4±0.4

Values are presented as percentages and mean±SD

Absolute numbers of each positive MRI finding of 30 volunteers are given in parentheses

In a study of 12 cadaveric MTP joints of the great toe, Theumann et al. [8] reported that a small distal central recess of the plantar plate was always visible on MR arthrography images and was not visible on MR images before arthrography. We observed a distal central recess, with a mean depth of 2.2 mm, in 77 % of cases. One might speculate that the high frequency of a distal central recess of the plantar plate might be diagnostically challenging in cases of patients referred for diagnostic imaging of dorsiflexion injuries of the capsuloligamentous complex of the first MTPJ, the so-called turf toe [1, 17–19, 28–30]. Theumann et al. found that the plantar plate of the first MTPJ was biconcave due to the embedded sesamoid bones and crista of the metatarsal head, as well as the flexor hallucis longus tendon in the middle, between the medial and lateral heads of the flexor hallucis brevis tendons. Therefore, the plantar plate of the first MTPJ is similar to the two distinct medial and lateral main longitudinal bundles of the plantar plate of the lesser MTPJs [8, 31].

A distal dorsal recess was observed in 87 % of images in the present study. Surprisingly, this distal dorsal recess of the first MTP joint is not described in the current literature. However, this recess is visible on a sagittal T1-weighted MR arthrography image in a study by Theumann et al. [8], as shown in Fig. 3. A similar distal dorsal recess was described as a distal phalangeal bare area by Mohana-Borges et al. [32] in a report regarding normal MRI anatomy of the lesser metatarsophalangeal joints in cadavers. Bade et al. [33] distinguished a distal dorsal recess of metacarpophalangeal joints II to V in 62 % (43/69) of images on conventional arthrograms.

Fig. 7 32-year-old male volunteer. The *open arrow* indicates a small distal central recess of the plantar plate of the left first metatarsophalangeal asymptomatic joint on a sagittal intermediate-weighted MR image with fat suppression. The *arrow* points to the distal dorsal recess

The acquisition time for MRI sequences with a dedicated 1.5-Tesla MRI scanner was 38:09 minutes. Based on our experience, the acquisition time for the dedicated extremity 1.5-Tesla MRI scanner is approximately 25 % longer than that of a standard whole-body 1.5-Tesla MRI scanner. The MRI sequences in this study were developed at our institution as routine MRI protocol for daily clinical imaging of the forefoot, including high-resolution images dedicated to the first MTPJ.

In summary, cartilage defects, bone marrow oedema-like signal changes, subchondral cysts, plantar recesses, and distal dorsal recesses were common findings in MR examinations of the first MTPJ in asymptomatic volunteers. However, cartilage defects of the first metatarsal head and in the metatarsosesamoid compartment were rare. The collateral ligaments were often heterogeneous in structure and showed increased signal intensity, whereas tendons in the majority of cases demonstrated low signal intensity. These observations should be considered in MR examinations of symptomatic cases.

Acknowledgments The scientific guarantor of this publication is Tobias J. Dietrich, MD, Radiology, Orthopedic University Hospital Balgrist, University of Zurich, Forchstrasse 340, CH-8008 Zurich, Switzerland. The authors of this manuscript declare no relationships with any companies whose products or services may be related to the subject matter of the article. The authors state that this work has not received any funding. No complex statistical methods were necessary for this paper. Institutional review board approval was obtained. Written informed consent was obtained from all subjects (volunteers) in this study. No study subjects and no cohorts have been reported or published previously. Methodology: prospective, observational, performed at one institution.

Conflict of interest No conflict of interest declared.

References

1. Ashman CJ, Klecker RJ, Yu JS (2001) Forefoot pain involving the metatarsal region: differential diagnosis with MR imaging. Radiographics 21:1425–1440

2. Sanders TG, Rathur SK (2008) Imaging of painful conditions of the hallucal sesamoid complex and plantar capsular structures of the first metatarsophalangeal joint. Radiol Clin North Am 46:1079–1092
3. Karasick D, Schweitzer ME (1998) Disorders of the hallux sesamoid complex: MR features. Skeletal Radiol 27:411–418
4. Schweitzer ME, Maheshwari S, Shabshin N (1999) Hallux valgus and hallux rigidus: MRI findings. Clin Imaging 23:397–402
5. Nwawka OK, Hayashi D, Diaz LE et al (2013) Sesamoids and accessory ossicles of the foot: anatomical variability and related pathology. Insights Imaging 4:581–593
6. Prescott JW, Yu JS (2012) The aging athlete: part 1, "boomeritis" of the lower extremity. AJR 199:W294–W306
7. Michelson J, Dunn L (2005) Tenosynovitis of the flexor hallucis longus: a clinical study of the spectrum of presentation and treatment. Foot Ankle Int 26:291–303
8. Theumann NH, Pfirrmann CW, Mohana Borges AV, Trudell DJ, Resnick D (2002) Metatarsophalangeal joint of the great toe: normal MR, MR arthrographic, and MR bursographic findings in cadavers. J Comput Assist Tomogr 26:829–838
9. Erickson SJ, Rosengarten JL (1993) MR imaging of the forefoot: normal anatomic findings. AJR 160:565–571
10. Lepage-Saucier M, Linda DD, Chang EY et al (2013) MRI of the metatarsophalangeal joints: improved assessment with toe traction and MR arthrography. AJR 200:868–871
11. Shortt CP (2010) Magnetic resonance imaging of the midfoot and forefoot: normal variants and pitfalls. Magn Reson Imaging Clin N Am 18:707–715
12. Karasick D, Wapner KL (1990) Hallux valgus deformity: preoperative radiologic assessment. AJR 155:119–123
13. Weir JP (2005) Quantifying test-retest reliability using the intraclass correlation coefficient and the SEM. J Strength Cond Res 19:231–240
14. Landis JR, Koch GG (1977) An application of hierarchical kappa-type statistics in the assessment of majority agreement among multiple observers. Biometrics 33:363–374
15. Viera AJ, Garrett JM (2005) Understanding interobserver agreement: the kappa statistic. Fam Med 37:360–363
16. Kadakia AR, Molloy A (2011) Current concepts review: traumatic disorders of the first metatarsophalangeal joint and sesamoid complex. Foot Ankle Int 32:834–839
17. Waldrop NE, Zirker CA, Wijdicks CA, Laprade RF, Clanton TO (2013) Radiographic evaluation of plantar plate injury: an in vitro biomechanical study. Foot Ankle Int 34:403–408
18. Lucas DE, Philbin T, Hatic S (2014) The plantar plate of the first metatarsophalangeal joint: an anatomical study. Foot Ankle Spec 108–112
19. George E, Harris AH, Dragoo JL, Hunt KJ (2014) Incidence and risk factors for turf toe injuries in intercollegiate football: data from the national collegiate athletic association injury surveillance system. Foot Ankle Int 35:108–115
20. Yu JS, Tanner JR (2002) Considerations in metatarsalgia and midfoot pain: an MR imaging perspective. Semin Musculoskelet Radiol 6: 91–104
21. Unger K, Rahimi F, Bareither D, Muehleman C (2000) The relationship between articular cartilage degeneration and bone changes of the first metatarsophalangeal joint. J Foot Ankle Surg 39:24–33
22. Smith SE, Landorf KB, Gilheany MF, Menz HB (2011) Development and reliability of an intraoperative first metatarsophalangeal joint cartilage evaluation tool for use in hallux valgus surgery. J Foot Ankle Surg 50:31–36
23. Bock P, Kristen KH, Kröner A, Engel A (2004) Hallux valgus and cartilage degeneration in the first metatarsophalangeal joint. J Bone Joint Surg (Br) 86:669–673
24. Buck FM, Grehn H, Hilbe M, Pfirrmann CW, Manzanell S, Hodler J (2009) Degeneration of the long biceps tendon: comparison of MRI with gross anatomy and histology. AJR 193:1367–1375
25. Bydder M, Rahal A, Fullerton GD, Bydder GM (2007) The magic angle effect: a source of artifact, determinant of image contrast, and technique for imaging. J Magn Reson Imaging 25:290–300
26. Frankel JP, Harrington J (1990) Symptomatic bipartite sesamoids. J Foot Surg 29:318–323
27. Zanetti M, Bruder E, Romero J, Hodler J (2000) Bone marrow edema pattern in osteoarthritic knees: correlation between MR imaging and histologic findings. Radiology 215:835–840
28. Tewes DP, Fischer DA, Fritts HM, Guanche CA (1994) MRI findings of acute turf toe. A case report and review of anatomy. Clin Orthop Relat Res 304:200–203
29. Yao L, Cracchiolo A, Farahani K, Seeger LL (1996) Magnetic resonance imaging of plantar plate rupture. Foot Ankle Int 17:33–36
30. Rodeo SA, O'Brien S, Warren RF, Barnes R, Wickiewicz TL, Dillingham MF (1990) Turf-toe: an analysis of metatarsophalangeal joint sprains in professional football players. Am J Sports Med 18: 280–285
31. Deland JT, Lee KT, Sobel M, DiCarlo EF (1995) Anatomy of the plantar plate and its attachments in the lesser metatarsal phalangeal joint. Foot Ankle Int 16:480–486
32. Mohana-Borges AV, Theumann NH, Pfirrmann CW, Chung CB, Resnick DL, Trudell DJ (2003) Lesser metatarsophalangeal joints: standard MR imaging, MR arthrography, and MR bursography—initial results in 48 cadaveric joints. Radiology 227:175–182
33. Bade H, Koebke J, Nieden A (1997) Radiologic anatomy of the metacarpophalangeal joints II to V. Surg Radiol Anat 19:323–327